Cloud screening and quality control algorithms for the AERONET database

A.Smirnov[1,2], B.N.Holben[1], T.F.Eck[1,3], O.Dubovik[1,2], I.Slutsker[1,2]

[1] NASA Goddard Space Flight Center, Biospheric Sciences Branch, Greenbelt, Maryland

[2] Science Systems and Applications, Inc., Lanham, Maryland

[3] Raytheon ITSS, Lanham, Maryland

Abstract

Automatic globally distributed networks for monitoring aerosol optical depth provide measurements of natural and anthropogenic aerosol loading important in many local and regional studies as well as global change research investigations. The strength of such networks relies on imposing a standardization of measurement and processing allowing multi year and large scale comparisons. The development of the Aerosol Robotic Network (AERONET) for systematic ground based sunphotometer measurements of aerosol optical depth is an essential and evolving step in this process. The growing database requires development of a consistent, reproducible and system-wide cloud screening procedure. This paper discusses the methodology and justification of the cloud-screening algorithm developed for the AERONET database. The procedure has been comprehensively tested on experimental data obtained in different geographical and optical conditions. These conditions include biomass burning events in Brazil and Zambia, hazy summer conditions in the Washington DC area, clean air advected from the Canadian Arctic, and variable cloudy conditions. For various sites our screening algorithm eliminates from ~20 to 50 percent of the initial data depending on cloud conditions. Certain shortcomings of the proposed procedure are discussed.

Introduction

The temporal and spatial distribution of natural and anthropogenic aerosol loading in the atmosphere has received sporadic scientific attention during the last half of this century as a measurement of regional air pollution and for the uncertain impact on global climate. During the last decade, renewed interest and greater understanding of aerosol processes have necessitated an emphasis in monitoring by ground and satellite based remote sensing approaches. Ground based systems, while generally considered simple, reliable and necessary to support satellite retrieval methodology through validation programs, have lacked consistent long term support and suffered from poor measurement and processing methodology resulting in fragmented data sets that are difficult to use for most scientific assessments (Forgan et al., 1994). Several automatic aerosol measurement networks have imposed a measurement standardization (Forgan, private communication, 1998; Holben et al., 1998; Takamura, private communication, 1998; Michalsky et al., 1994; GAW, 1992) for their respective instruments. Measurement, processing, and quality assurance is evolving for all networks. One critical aspect of this evolutionary process, common to all aerosol optical depth retrievals from sun photometry networks, is separation of cloud affected data from cloud free data.

For manual instruments, it is in principle very easy to deal with the presence of clouds. Human observers can detect clouds based on subtle textural and spatial patterns and therefore do not make observations under those conditions (Kaufman and Fraser, 1983). Deployment of automatic instruments poses the problem of defining an effective cloud screening procedure. In dealing with one or two instruments for relatively short time periods, it is possible to perform “subjective” screening by a human analyst (see, e.g. Markham et al., 1997; Smirnov et al., 1994; Ahern et al., 1991). But it would, however, be time and labor consuming to perform similar “manual” cloud screening of multi-year records for any significant number of instruments. Further argument for automatic cloud screening is that human observers can be inconsistent in their cloud detection decisions.

Procedures should be computerized and at the same time generalized as much as possible to be able to handle data sets associated with various and sometimes absolutely different types of aerosol. Harrison and Michalsky (1994) have developed an objective analysis algorithm for their Langley regressions. This algorithm was, however, designed for a multi-filter rotating shadow-band radiometer. Instruments of this type have their own methodological singularities and hence require a different measurement protocol.

The AERONET federated network is the most globally distributed ground based system resulting in a database of widely variable atmospheric conditions. AERONET imposes standardization for measurement protocol, data processing and calibration. By necessity, a reliable and physically admissible automatic cloud screening procedure is fundamental for the success of the program.

The automatic sun/sky CIMEL radiometer CE-318 acquires data regardless of sky conditions. The radiometer makes only two basic measurements, either direct sun or diffuse sky radiances, both within several programmed sequences. The direct sun measurements pose the most difficult screening problem and are the subject of this paper.

The direct sun measurements are acquired in approximately 10 seconds across eight spectral bands which are located between 340 and 1020 nm (440, 675, 870, 940 and 1020 nm are standard). A sequence of three such measurements are taken 30 seconds apart to yield a triplet observation per wavelength. Triplet observations are made during morning and afternoon Langley calibration sequences at precomputed optical airmass values and at standard 15-minute intervals in between. The temporal variation of cloud optical depths is typically greater than that of aerosols causing an increase in the observable variation in the triplets (Holben et al., 1998).

We used two major criteria in our cloud screening procedure. First, we retained stable triplets (all wavelengths) in order to eliminate high frequency changes. Second, we eliminated rapid temporal optical depth diurnal variations (“spikes”) between selected triplets by applying a root mean square second derivative threshold. From a physical point

of view, $\tau_a(\lambda)$ cannot undergo large rapid changes (except in narrow plumes) and some smoothness in time and space can be expected. The smoothness criterion is based on the idea of limiting sudden increases and decreases of optical depth.

The procedure was tested on experimental data obtained in different geographical and optical conditions. These include biomass burning events in Brazil and Zambia, hazy summer conditions in the Washington DC area, clean air advected from the Canadian Arctic, and variable cloudy conditions. A certain degree of preference was given to several cases when observer's remarks were available. For a variety of sites our screening algorithm eliminated from ~20 to 50 percent of the initial data. Overall, with the exception of cases involving very thin stable cirrus, the cloud-screening algorithm described below produced promising results.

Algorithm description

In this section we describe our cloud-screening algorithm and present a few examples of the data before and after screening.

1. Data quality checks.

If the aerosol optical depth is lower than -0.01 at any wavelength we do not accept the corresponding τ_a . We eliminate only measurements in that particular channel where τ_a <-0.01, while preserving τ_a in all channels that yielded optical depths higher than -0.01 (Figure 1).

Negative values of aerosol optical depth are not physical. However, these low optical depths might be caused by calibration, temperature correction at the wavelength 1020 nm, atmospheric pressure and column ozone amount uncertainties.

Values of stratospheric background aerosol optical depth in undisturbed conditions are about 0.005 at 500 nm, as summarized by Russell et al. (1993). The Angstrom parameter for background stratospheric conditions is about 1.6 (McClatchey et al., 1982). Spectrally

this results in a change of τ_a from 0.009 at 340 nm to 0.002 at 1020 nm. These values are very close to our overall accuracy estimates for freshly calibrated "reference" instruments (Eck et al., 1999) (τ_a uncertainties are higher for the field instruments). Therefore, under the clearest (lowest τ_a) conditions, with little tropospheric aerosol present, the uncertainty in computed τ_a may result in slightly negative τ_a values, whose differences are still statistically insignificant from zero.

Because measurements made during low sun elevation angles have a higher chance of cloud contamination (due to a decreased probability gap for vertically developed clouds) and in order not to unduly weight daily averages with the higher frequency data acquired during the Langley sequence (Holben et al., 1998), $\tau_a(\lambda)$ for air mass m > 5 are not considered in the screened data base. However, the initial database remains intact and available for low sun data analysis.

2. Triplet stability criterion.

A measurement triplet taken with the CIMEL sun/sky radiometer consists of 3 measurements, each made 30 seconds apart over a total of a 1 minute period. We presume that the aerosol optical depth in the total atmospheric column should vary by less than 0.02 within one triplet for all wavelengths if the atmosphere is to be considered stable and cloud free. In other words, $(\tau_{max} - \tau_{min}) < 0.02$ for triplets defines τ_i^{good} (eliminate high frequency temporal unstability). When a triplet is identified as good, we use the average τ_a value of the 3 measurements as our cloud screened value of τ_a . If the triplet variability exceeds our threshold at any wavelength then we eliminate the measurement at all wavelengths completely.

Figures 2a and 2b present an example of aerosol optical depth diurnal variability (at Goddard Space Flight Center (GSFC) in Greenbelt, MD) before and after application of the triplet criterion. Visual observations indicate thin cirrus clouds were developing throughout the day, becoming thicker about 1700 GMT, then dissipating and developing again. Several "cloud contaminated" points in Fig.2b not eliminated by the criterion of triplet stability, were nonetheless screened out after the criteria discussed in the next sections were applied.

The justification for the 0.02 threshold is based on empirical evidence. Since atmospheric variability will dominate the triplet test we analyzed the triplet variability in various optical conditions we believed to be cloudless (dust outbreaks, maritime, rural and urban aerosol). For such conditions the variability of optical depth within one minute at any wavelength for $\tau_a<0.7$ was always lower than 0.02. When optical depth is high (biomass burning, extremely hazy conditions etc.) we allow triplet variability to be a maximum of $0.03\tau_a$. Thus, we accept measurements with a triplet variability of either 0.02 or $0.03\tau_a$ (whichever is higher). Empirically we found that in conditions of biomass burning and extremely high loading (optical depth higher than 2) normally $(\tau_{max} - \tau_{min}) < 0.03\tau_a$ at all wavelengths.

Figure 3a presents the results of optical depth measurements carried out in Litoya, Zambia during conditions of highly variable biomass burning (with smoke plumes imbedded in a regional haze). Measurements were made at intervals of 60 seconds during a 4 hour period in the presense of a human observer. The highly variable aerosol optical conditions may be considered as a "worst case scenario" for the triplet test. A single band of cirrus cloud was observed only once at about 1235 GMT. Due to the very high aerosol loading some cirrus might have gone undetected, but they would have been of relatively low optical depth. As one would expect for a smoke aerosol the most variable channel appears to be 340 nm. At the longest wavelengths, the aerosol optical depth shows much less variability. This is

typical for conditions of biomass burning, since the size distribution is dominated by small particles. The computed threshold of the maximum variability (i.e. $0.03\tau_a$(340 nm)) and the corresponding "measured" τ_a(340 nm) range over a one minute period is presented in Figure 3b. Only in 8% of the measurements does the "measured" variability exceed the computed ("assumed") threshold at this most sensitive wavelength. We would like to reiterate that aerosol optical conditions in Litoya were highly variable on this date due the presence of nearby smoke plumes.

We made additional tests of our triplet variability criteria on measurements made in conditions of biomass burning and high aerosol loading. Excluding all the data with low $\tau_a(\lambda)$ (using τ_a(500 nm) <0.40 as a boundary condition) we considered measurements of aerosol optical depth made in Mongu, Zambia during several months in 1997. Overall, 1225 measurements were tested for triplet variability. Fig.4a presents a histogram of the triplet variability ranges, both "measured" and "assumed" at the 340 nm wavelength. The most important conclusion that we are able to make is that our assumed threshold of $0.03\tau_a$ allows more triplet variability than required in most cases. Indeed, our "assumed" range histogram is shifted with respect to the "measured" histogram and in almost 40% of all cases considered the measured triplet range is smaller than 0.02. Figure 4b presents a histogram of the τ_a(340 nm) values for the corresponding data set. More than 85% of the τ_a(340 nm) values were higher than 0.75, due to the criterion of τ_a(500 nm) >0.40 and due to the fact that the wavelength exponent of smoke typically ranges from 1.7-1.9.

3. Diurnal stability check.

If the standard deviation of the averaged aerosol optical depth at 500 nm (or 440 nm, if 500 nm is not available) for an entire day is less than 0.015 (after triplet variability screening), then we stop the screening and accept all the remaining measurements.

Because the estimated accuracy of our newly calibrated field instruments is about ±0.01 in τ_a (Holben et al., 1998) it is not necessary to check the rest of the data since the diurnal variability is less than or similar to the measurement accuracy.

4. Smoothness criteria.

The smoothness criterion (of a time series) is based on limiting the root mean square of the aerosol optical depth second derivative with time. The first derivative yields the rate of temporal change (both negative and positive). The second derivative defines the variability of that tendency and, consequently, it is very sensitive to the local oscillations of optical depth caused by clouds: the average second derivative increases substantially in the presence of such oscillations.

It should be noted that limiting the average derivatives of physical characteristics is traditionally used in methods of constrained inversion in remote sensing (e.g. see (Twomey, 1977)). There, such smoothness restrictions are successfully applied in retrieving aerosol particle size distributions or atmospheric vertical profiles to eliminate artificial local oscillations related to error effects. In our cloud-screening algorithm we have adopted the smoothness evaluation strategy developed in the method of constrained inversion. Thus, we assume that a norm of the second derivative of optical depth with time should not exceed a certain threshold, i.e.

$$(D_2)^2 = \int_{t_1}^{t_2} \left(\frac{\partial^2 \tau(t)}{\partial t^2} \right)^2 dt \le D^2_{critic},$$

where D^2_{critic} is a priori defined and corresponds to the maximum expected variability of aerosol optical depth. In addition we restrict the logarithmic second derivative of optical depth (in a manner similar to the smoothness constraints employed by Dubovik et al. (1995)). The utilization of a logarithmic derivative ensures a coherent threshold D in cases

of both low and high optical depth. We feel that the use of absolute derivatives ($\frac{d^2\tau}{dt^2}$) would not be realistic inasmuch as one expects magnitude dependent fluctuations of optical depth in clear to very hazy conditions. Fixed thresholds in logarithmic space accordingly help to overcome this problem. This is clearly seen in the simple relationship between the logarithmic and linear derivatives:

$$\frac{\mathbf{d}\ln\tau(\mathbf{t})}{\mathbf{dt}} = \frac{1}{\tau(\mathbf{t})}\frac{\mathbf{d}\tau(\mathbf{t})}{\mathbf{dt}}$$

Taking into account that the measurements of optical depth are taken in *n* discrete moments of time we used differences instead of analytical derivatives. Finally, for operational purposes, we defined an index D (first derivatives difference) similar to the norm of second derivative D_2:

$$D = \sqrt{\frac{1}{(\mathbf{n}-2)}\sum\left[\frac{\mathbf{Ln}\tau_{\mathbf{i}}-\mathbf{Ln}\tau_{\mathbf{i}+1}}{\mathbf{t_i}-\mathbf{t_{i+1}}} - \frac{\mathbf{Ln}\tau_{\mathbf{i}+1}-\mathbf{Ln}\tau_{\mathbf{i}+2}}{\mathbf{t_{i+1}}-\mathbf{t_{i+2}}}\right]^2} \leq 16$$

If D>16 we find the term with the maximum input to D and eliminate the maximum optical depth associated with it. We then apply the diurnal stability check again (Section 3) and repeat it every time we reject a measurement according to our smoothness criteria.

When the number of measurements in a day is reduced to only 1 or 2, we then reject that day. When the number of measurements remaining is 3 (after criteria 1 through 3 have been applied) we apply the smoothness criteria. If D>16 we reject that day. Otherwise we accept it and go to the next criterion.

Our threshold ($D \leq 16$) is founded on experimental data obtained in various optical conditions: biomass burning aerosol, extremely hazy urban/industrial conditions, clean maritime and background continental air. Fig.5a shows an example based on several hundred measurements in Cuiaba, Brazil and at Goddard Space Flight Center in Greenbelt, MD. Parameter D, as one can see, is somewhat dependent on τ_a(500 nm) with higher values at lower τ_a. Empirically we found that the number of points with $D>20$ may vary depending on the data set considered. But the number of points within the $D<20$ population with $16<D\leq20$ was consistently ~5%. D is less than 16 in about 95% of cases with $D<20$ and usually less than 10 when τ_a(500 nm) is higher than 0.5. The corresponding histogram is shown in Fig.5b.

We would like to emphasize that application of the "D" (second derivative) criterion does not bias our daily averages. For the GSFC database, we analyzed about 850 days and found that the smoothness criterion was invoked on only about 10% of those days. Fig.6a presents a histogram that shows the number of instantaneous τ_a measurements per day eliminated by the "D" criterion (on those days when it was invoked). In the overwhelming majority of cases, the "D" criterion eliminated only one or two measurements per day. Fig.6b shows that for the days affected by the smoothness criterion (i.e.10% of all the days), only a small number of the associated daily averages show τ_a(500 nm) differences (before and after the D criterion) higher than 0.02. Therefore, the application of the second derivative screening has relatively little impact on the daily τ_a average for the majority of days.

Fig.7 presents an example of the application of the smoothness criteria to real data and Fig.7b shows how the data with large temporal changes ("spikes") have been eliminated.

5. Three standard deviation criteria.

In this step we check if any measurements fall outside of the 3σ range about the mean of τ_a(500 nm) as well as for the Angstrom parameter α (estimated using least-square regression in the 440-870 nm range), taken over the entire day (i.e. τ_a(500 nm) ± 3σ and α ± 3σ). For a normal distribution (see, for example, (Panofsky and Brier, 1968)), the probability of obtaining a value deviating from the mean of a given sample by more than 3σ is equal to 0.003. In other words, all measurements that differ from the mean by 3σ (or greater) could be considered as highly improbable and eliminated.

Discussion

Certain shortcomings of our screening algorithm are apparent. In order to create a scheme that is as general as possible, we did not impose any restrictions on the Angstrom parameter. A possible check for cloud contamination would be to confine the Angstrom parameter variability depending on site and prevailing type of aerosol. For example, in continental turbid conditions (aerosol optical depth higher than 0.5-0.7 at 500 nm) we could restrict α to be larger than, say, 0.5-0.7 for cloudless conditions. Measurements with almost neutral τ_a spectral dependence would thus be automatically deleted as cloud contaminated. However, such automatic filtering may work well for one site but not another. In addition it could jeopardize the detection of some unusual events, such as the large-scale transport of dust from Mongolia to the west coast of the United States (e.g. Tratt et al., 1999). Also, we may miss some interesting aerosol optical situations at sites, which do not conform to the statistics defined by the *apriori* knowledge of aerosol optical properties.

One more data quality check was done specifically for high turbidity conditions. In certain cases when aerosol optical depth was usually higher than 1.5 an out-of-band leakage artifact has been observed in the shortest wavelengths. The presence of parasitic light in the sunphotometer signal led to early morning and afternoon “drop-offs” in the diurnal behavior of aerosol optical depth. This simply means the signal was higher than it should be and hence the apparently anomalous low aerosol optical depths were registered. The essential difficulty induced by the presence of parasitic light in a sunphotometer signal is simply that the optical depth over wavelengths characteristic of the leakage band can be significantly different from the optical depth associated with the nominal filter band.

In dealing with this problem on a case by case basis we empirically found that if the measured voltage is smaller than 50 counts the measurement should be rejected. After weak signals associated with out-of-band leakage were removed the diurnal variability are realistic and in general much less susceptible to the influence of this obvious spectrally dependent signal artifact. It is worth noting, that we did not encounter this problem after deployment of the ion assisted deposition filters in 1997, which obviously have better blocking of parasitic out-of-band signal.

Fig.8 presents an example of the application of the cloud-screening algorithm to real data. The scattergram shows the variability of the Angstrom parameter for the unscreened (Fig.8a) and cloud-screened (Fig.8b) instantaneous aerosol optical depth measurements taken in Los Fierros, Bolivia from May 4 till September 1, 1998. This measurement period covers the pre-burning and burning seasons, thus a variety of optical conditions were observed. One may observe from Fig.8 that the obvious cloud contaminated data were eliminated since cloud exhibits Angstrom parameter values near zero or even negative due to the large droplet/crystal sizes. We would like to emphasize again, that we did not impose any specific limitations on the Angstrom parameter but only on temporal variability of optical depth. Approximately 75% of the initial data remain after the cloud screening.

We would like to make a few final comments regarding our cloud-screening and quality control algorithm. Our paper deals with the quality control and cloud screening tools for a specific database and a specific instrument (CIMEL sun/sky radiometer) and associated measurement sequence. Therefore this is not a generalized model, which would be applied to all types of τ_a measurement systems.

Error analysis of individual measurements is not the focus of this paper. However Schmid et al. (1999) show that agreement in aerosol optical depth measured by CIMEL and other instruments in field experimental conditions is within 0.015 (rms). Holben et al. (1998) and Eck et al. (1999) present careful assessments of the overall accuracy of the CIMEL sunphotometer due to calibration uncertainty and lack of surface pressure data and actual ozone column amount. Typically, the total uncertainty in $\tau_a(\lambda)$ for a newly calibrated field instrument for cloud-free conditions is $<\pm0.01$ for $\lambda\geq440$ nm and $<\pm0.02$ for shorter wavelengths. This by no means should be construed to mean an instrument from the field after pre- and post- field calibration, reprocessing and filtering through the cloud-screening algorithm would have accuracy $\leq\pm0.01$ in aerosol optical depth for all wavelengths. The final accuracy depends in part on the field history, including mechanical, electrical and optical integrity during the field measurements.

Summary

The principal conclusions drawn from this study can be summarized as follows:

1. A cloud-screening algorithm for the AERONET aerosol optical depth database was created, comprehensively tested and implemented. The corresponding flow diagram (Fig.1) describes the procedure. The two principal threshold criteria are both related to temporal variations of τ_a. One (the triplet stability criterion) is applied to short time period variability

(one minute) and the other (smoothness criterion) to hourly and diurnal time period variations of τ_a.

2. The conditions imposed on aerosol optical depth diurnal variability are not excessive and do not strongly bias the computation of daily averages. The proposed algorithm can be applied to any site of the AERONET network inasmuch as the paradigm was developed across an ensemble of network sites and aerosol conditions.

3. Since temporal variations of τ_a are identified as cloud contamination, it is noted that some cases of variable aerosol plumes will be screened by this algorithm. Conversely, stable uniform cloud will pass the algorithm thresholds and be identified as cloud free. However, we emphasize that the original (non-screened) data base for AERONET sites is also available on the web page (http://aeronet.gsfc.nasa.gov:8080/).

Acknowledgments

The authors thank Dr. Diane Wickland and Dr. Robert Curran of NASA Headquarters and Dr. Michael King of the EOS Project Science Office for their support. The authors would like to thank R.Fraser, Y.Kaufman, D.Tanre and N.O'Neill for fruitful discussions of certain issues. The authors would also like to acknowledge the constructive criticism of anonymous reviewers.

References

Ahern, F.J., Gauthier, R.P., Teillet, P.M., Sirois, J., Fedosejevs, G., and Lorente, D. (1991), Investigation of continental aerosols with high-spectral-resolution solar-extinction measurements, *Appl. Opt.* 30: 5276-5287.

Dubovik , O.V., Lapyonok, T.V., and Oshchepkov, S.L. (1995), Improved technique for data inversion: optical sizing of multicomponent aerosols, *Appl. Opt*. 34: 8422-8436.

Eck, T.F., Holben, B.N., Reid, J.S., Dubovik, O., Smirnov, A., O'Neill, N.T., Slutsker, I., and Kinne, S. (1999), The wavelength dependence of the optical depth of biomass burning, urban and desert dust aerosols, *J.Geoph.Res.*, *104*, 31,333-31,350, 1999.

Forgan, B.W., DeLuisi, J.J., Hicks, B.B., and Rusina, E.N. (1994), Report on the measurements of atmospheric turbidity in BAPMoN, *Rep. WMO*, No. 94, Geneva.

GAW (1992), *GAW measurement guide*, WMO/GAW Draft Report.

Harrison, L., and Michalsky, J. (1994), Objective algorithms for the retrieval of optical depths from ground-based measurements, *Appl.Opt*. 33: 5126-5132.

Holben, B.N., et al. (1998), AERONET - a federated instrument network and data archive for aerosol characterization, *Rem.Sens.Env*. 66, 1-16.

Kaufman, Y.J., and Fraser, R.S. (1983), Light extinction by aerosols during summer air pollution, *J. Clim.Appl. Met*. 22: 1694-1706.

Markham, B.L., Schafer, J.S., Holben, B.N., and Halthore, R.N. (1997), Atmospheric aerosol and water vapor characteristics over north central Canada during BOREAS, *J.Geoph.Res*. 102: 29,737-29,745.

McClatchey, R.A., Bolle, H.J., and Kondratyev, K.Ya. (1982), A preliminary cloudless standard atmosphere for radiation computation, *Int. Radiation Com. Rep.*, Boulder, Colorado, USA, p.p.78-104, 1982.

Michalsky, J.J., Schlemmer, J.A., Larson, N.R., Harrison, L.C., Berkheiser III, W.E., and Laulainen, N.S. (1994), Measurement of the seasonal and annual variability of total column aerosol in a northeastern US network, in *Proceedings of the International Specialty Conference Aerosols and Atmospheric Optics: Radiative Balance and Visual Air Quality*, Snowbird, Utah, USA, September 26-30, 1994, vol. A, pp. 247-258, Pittsburg, PA.

Panofsky, H.A., and Brier, G.W. (1968), *Some applications of statistics to meteorology*, 224 pp., The Pennsylvania State University, University Park, Pennsylvania.

Russell, P.B., et al. (1993), Pinatubo and pre-Pinatubo optical depth spectra: Mauna Loa measurements, comparisons, inferred particle size distributions, radiative effects, and relationship to lidar data, *J.Geophys.Res.* 98: 22,969-22,985.

Schmid, B., Michalsky, J., Halthore, R., Beauharnois, M., Harrison, L., Livingston, J., Russell, P.B., Holben, B.N., Eck, T.F., and Smirnov, A. (1999), Comparison of aerosol optical depth from four solar radiometers during the fall 1997 ARM Intensive Observation Period, *Geoph.Res.Let*., 26, 2725-2728.

Smirnov, A., Royer, A., O'Neill, N.T., and Tarussov, A. (1994), A study of the link between synoptic air mass type and atmospheric optical parameters, *J.Geophys.Res.*, 99: 20,967-20,982.

Tratt, D.M., Frouin, R.J., and Westphal, D.L. (1999), A Southern California perspective of the April, 1998 trans-Pacific Asian dust event, Proceedings, 10th Conference on Coherent Laser Radar, Mt. Hood, Ore., June 28 - July 2, 1999, 137-140.

Twomey, S. (1977), *Introduction to the mathematics of inversion in remote sensing and indirect measurements*, 243 pp., Elsevier, New York.

Figure captions.

Figure 1. Flow diagram describing the cloud-screening algorithm for the AERONET aerosol optical depth database.

Figure 2. Diurnal variability of aerosol optical depth on July 5, 1996 over GSFC, Greenbelt, Maryland, before (a) and after (b) screening criterion 2 (triplet stability) has been applied.

Figure 3. Time series of aerosol optical depth on August 29, 1997 over Litoya, Zambia, during conditions of smoke plumes (a) and corresponding “assumed” and “measured” variability range of τ_a(340 nm) over a one minute period (b).

Figure 4. Histogram of the “assumed” and “measured” triplet variability ranges at 340 nm for biomass smoke observations in Zambia in 1997 (a) and histogram of the corresponding aerosol optical depth at 340 nm (b).

Figure 5. Scattergram of parameter D versus aerosol optical depth at 500 nm from Cuiaba, Brazil and Goddard Space Flight Center observations (a) and corresponding histogram of the parameter D (b).

Figure 6. Histogram of the number of τ_a measurements within a day eliminated by the smoothness criterion for observations made at Goddard Space Flight Center (a) and histogram of the corresponding change in aerosol optical depth at 500 nm (b).

Figure 7. Diurnal variability of aerosol optical depth on November 5, 1995 over GSFC, Greenbelt, Maryland, before (a) and after (b) screening criterion 4 (smoothness criteria) has been applied.

Figure 8. Scattergram of the Angstrom parameter versus aerosol optical depth at 500 nm from Los Fierros, Bolivia observations before (a) and after (b) cloud-screening algorithm has been applied.

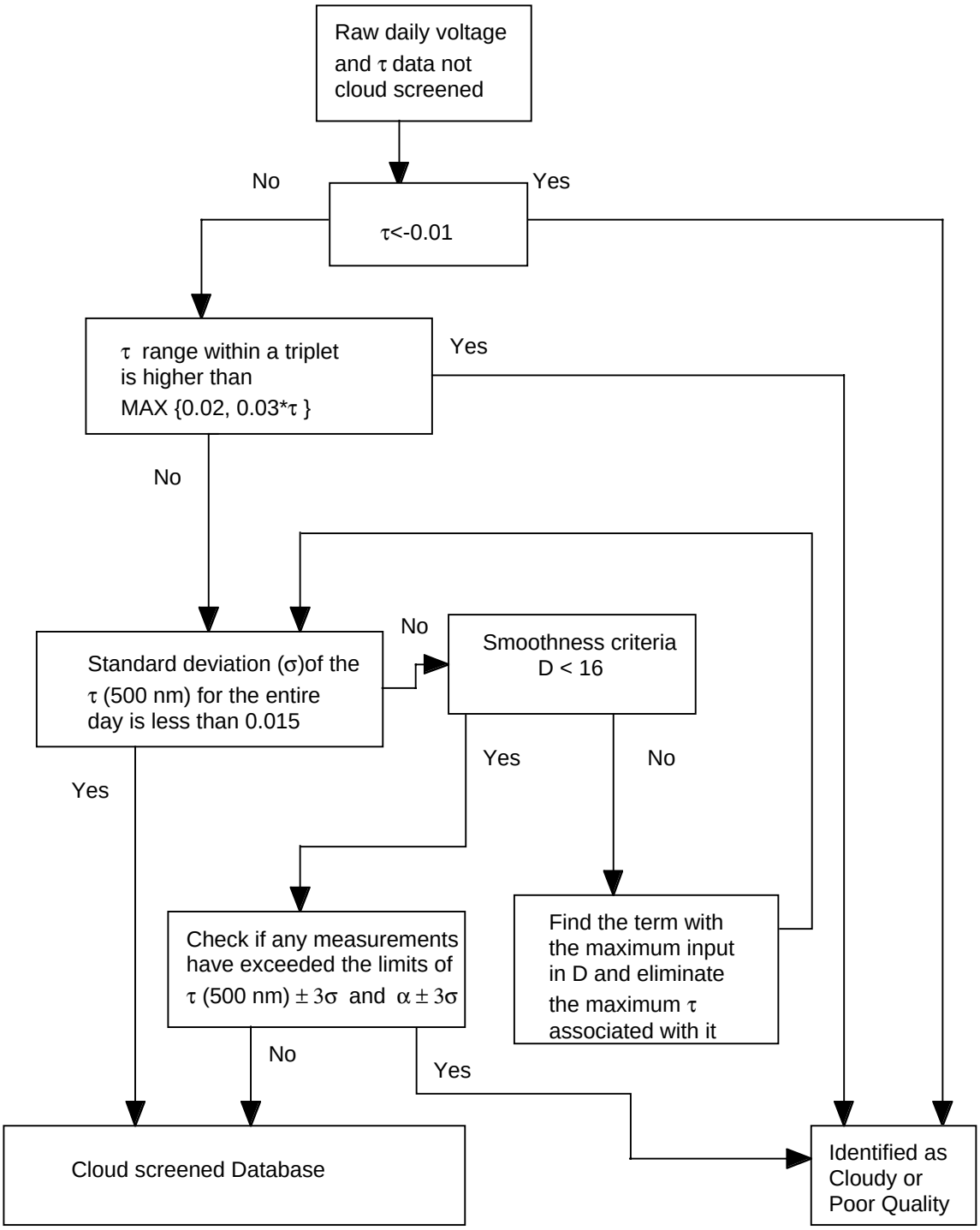
Raw daily voltage and τ data not cloud screened
No
Yes
τ<-0.01
τ range within a triplet is higher than MAX {0.02, 0.03*τ }
Yes
No
Standard deviation (σ)of the τ (500 nm) for the entire day is less than 0.015
No
Smoothness criteria D < 16
Yes
No
Yes
Check if any measurements have exceeded the limits of τ (500 nm) ± 3σ and α ± 3σ
Find the term with the maximum input in D and eliminate the maximum τ associated with it
No
Yes
Cloud screened Database
Identified as Cloudy or Poor Quality

Figure 2. Diurnal variability of aerosol optical depth on July 5, 1996 over GSFC, Greenbelt, Maryland, before (a) and after (b) screening criterion 2 (triplet stability) has been applied.

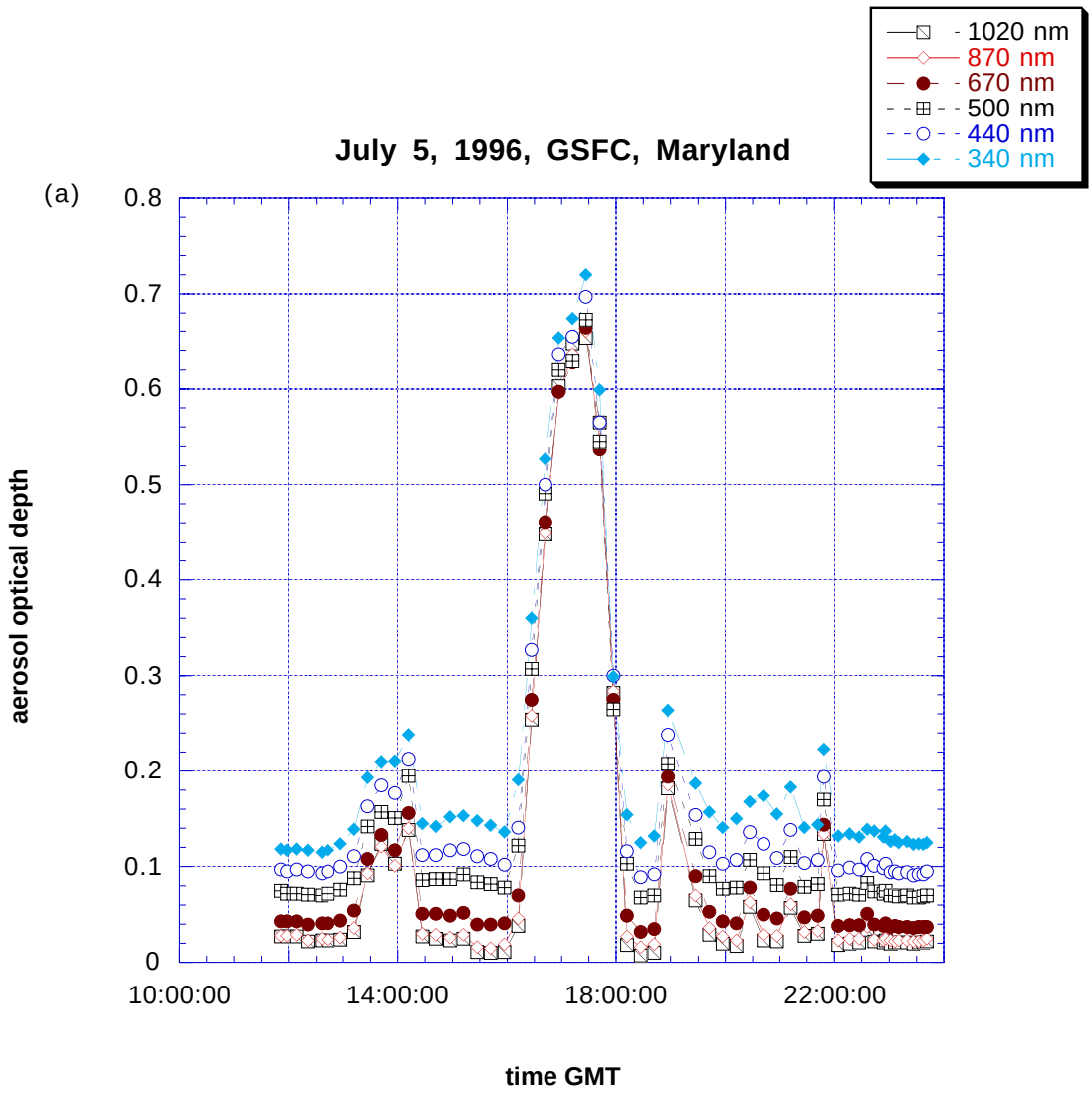

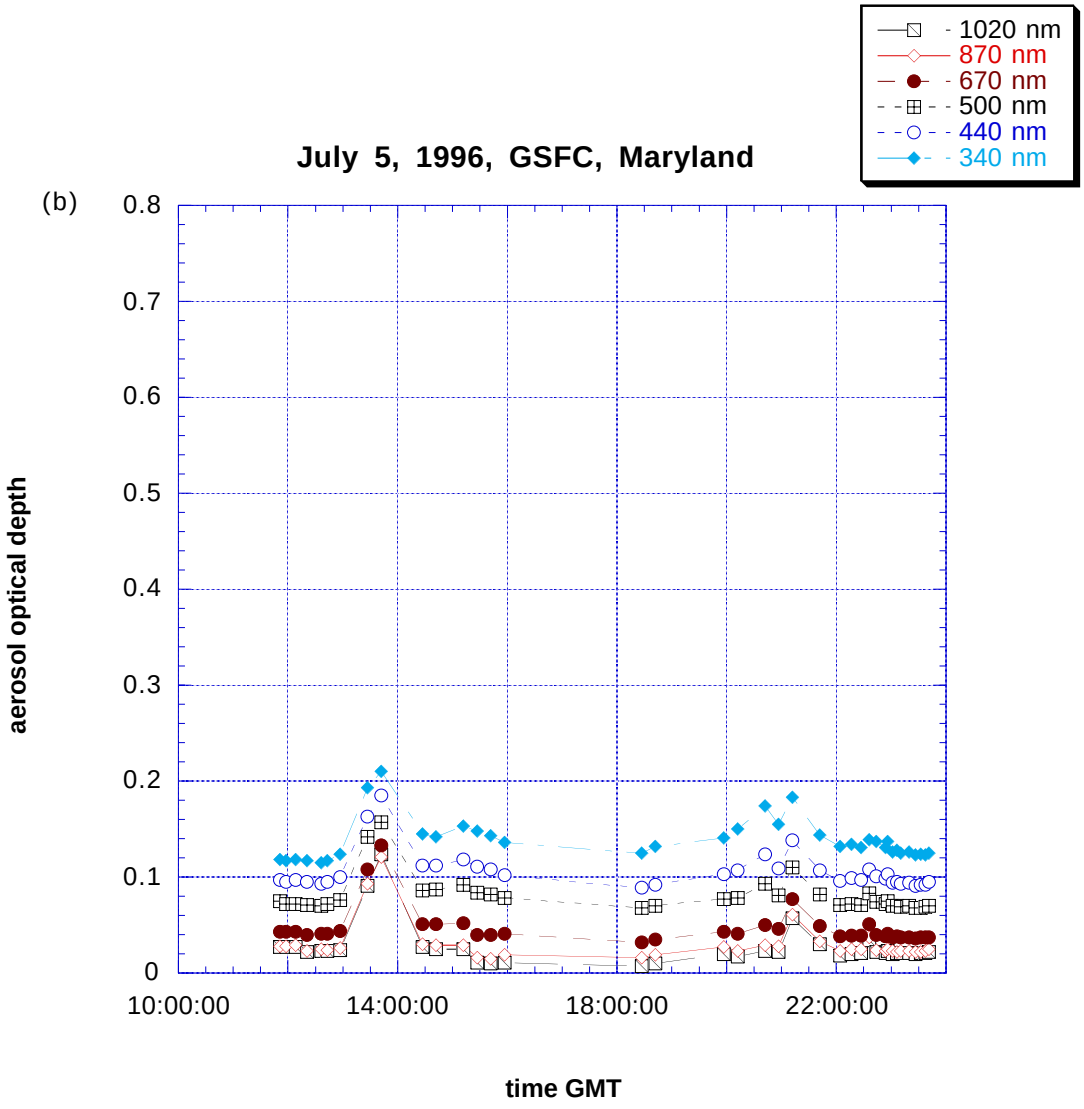
1020 nm
870 nm
670 nm
500 nm
440 nm
340 nm
July 5, 1996, GSFC, Maryland
(b)
0.8
0.7
0.6
0.5
0.4
0.3
0.2
0.1
0
aerosol optical depth
10:00:00
14:00:00
18:00:00
22:00:00
time GMT

Figure 3. Time series of aerosol optical depth on August 29, 1997 over Litoya, Zambia, during conditions of smoke plumes (a) and corresponding "assumed" and "measured" variability range of τ_a(340 nm) over a one minute period (b).

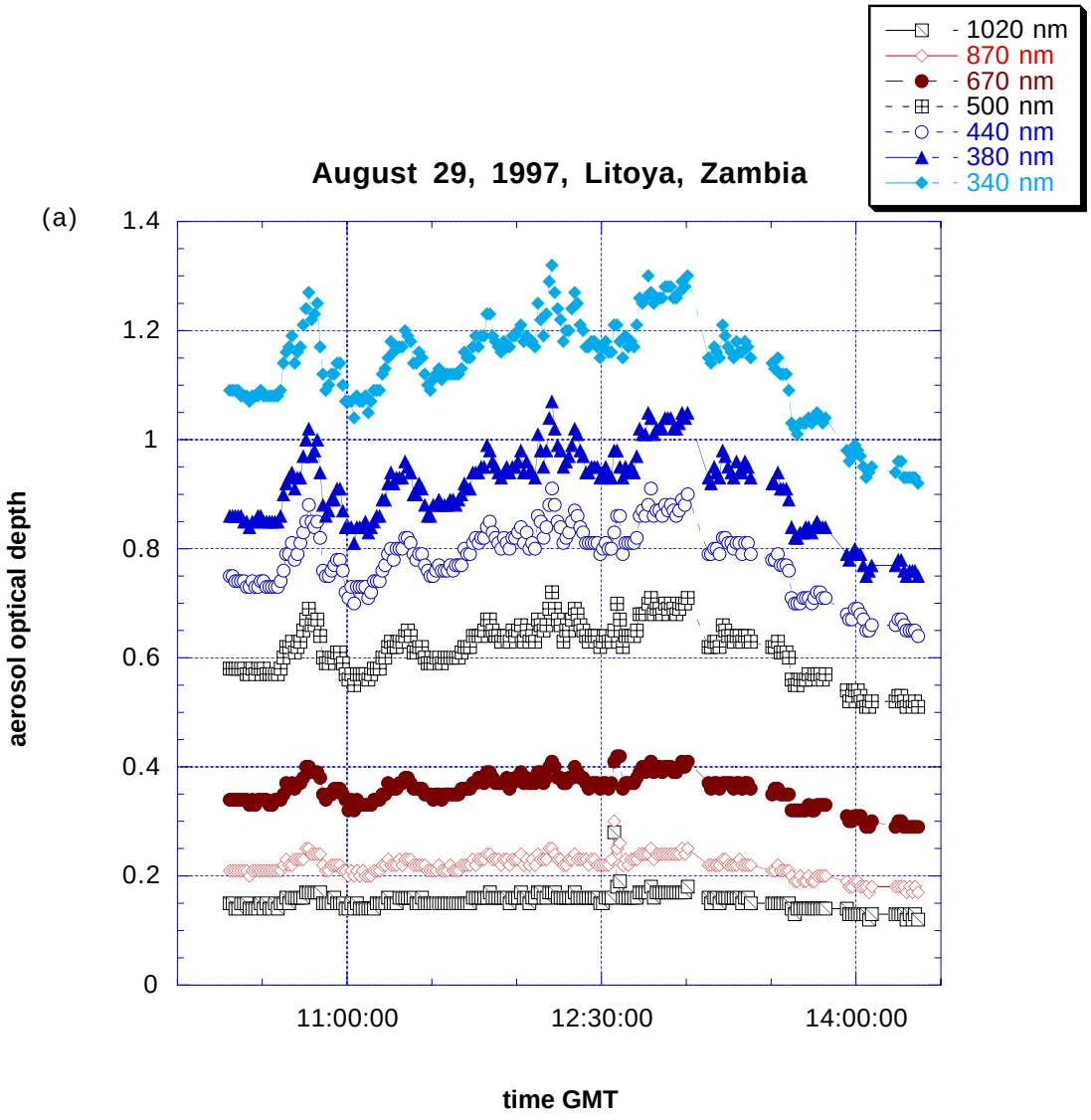

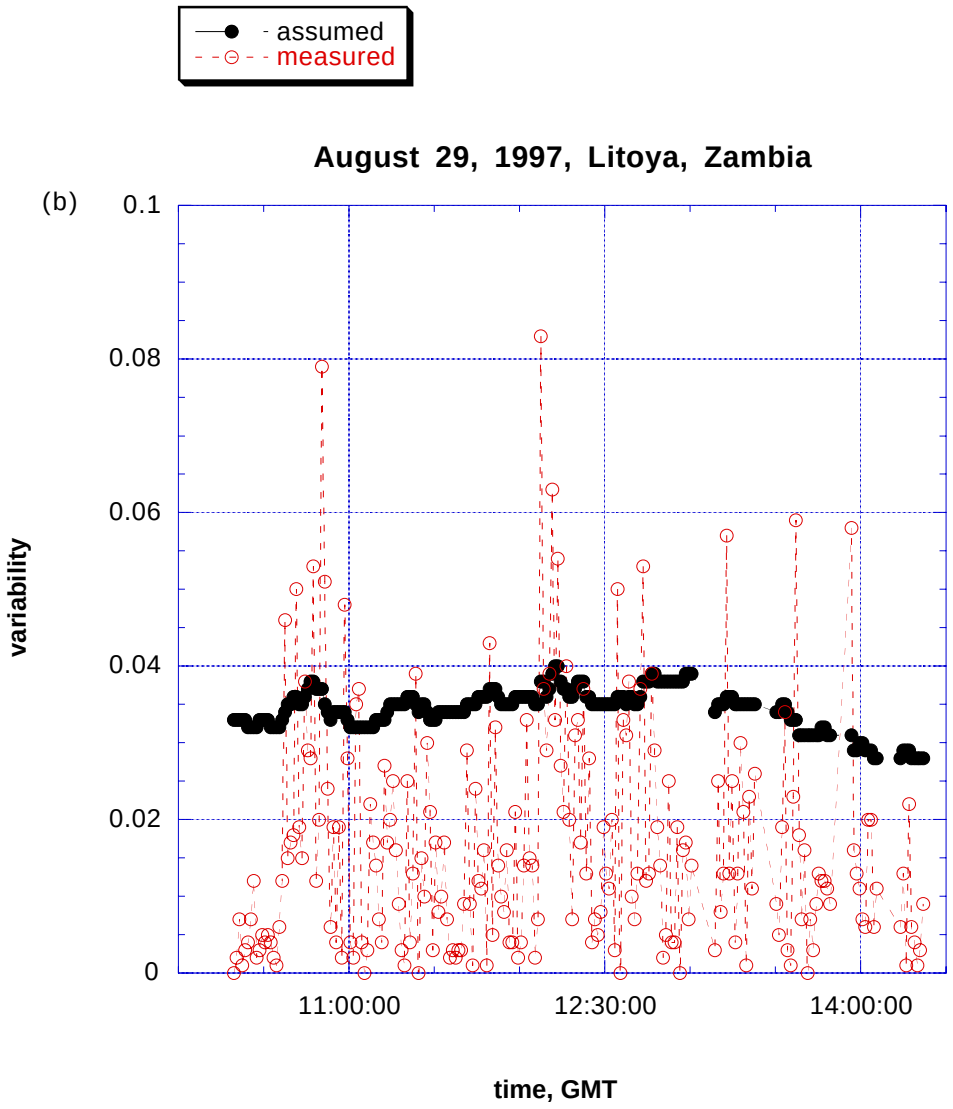
assumed
measured
August 29, 1997, Litoya, Zambia
(b)
0.1
0.08
0.06
0.04
0.02
0
variability
11:00:00
12:30:00
14:00:00
time, GMT

Figure 4. Histogram of the "assumed" and "measured" triplet variability ranges at 340 nm for biomass smoke observations in Zambia in 1997 (a) and histogram of the corresponding aerosol optical depth at 340 nm (b).

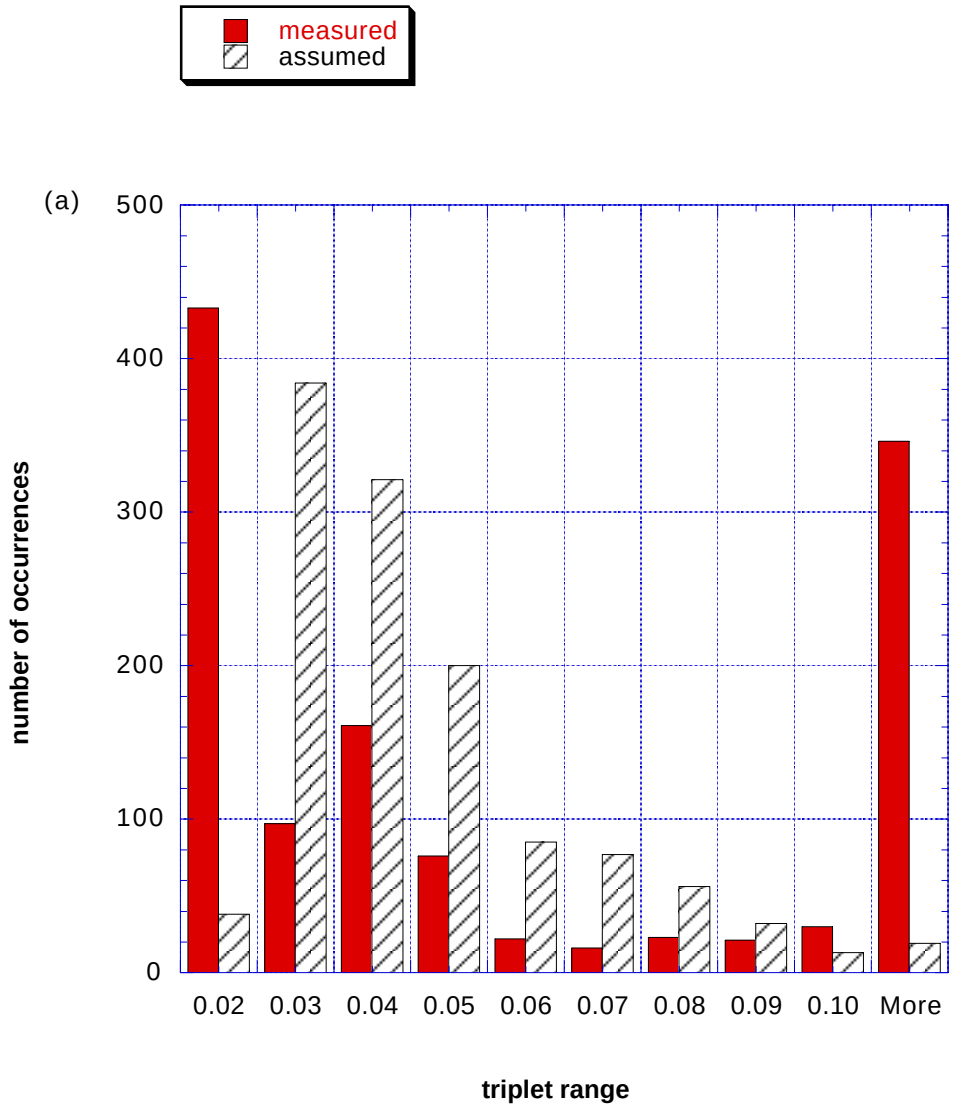

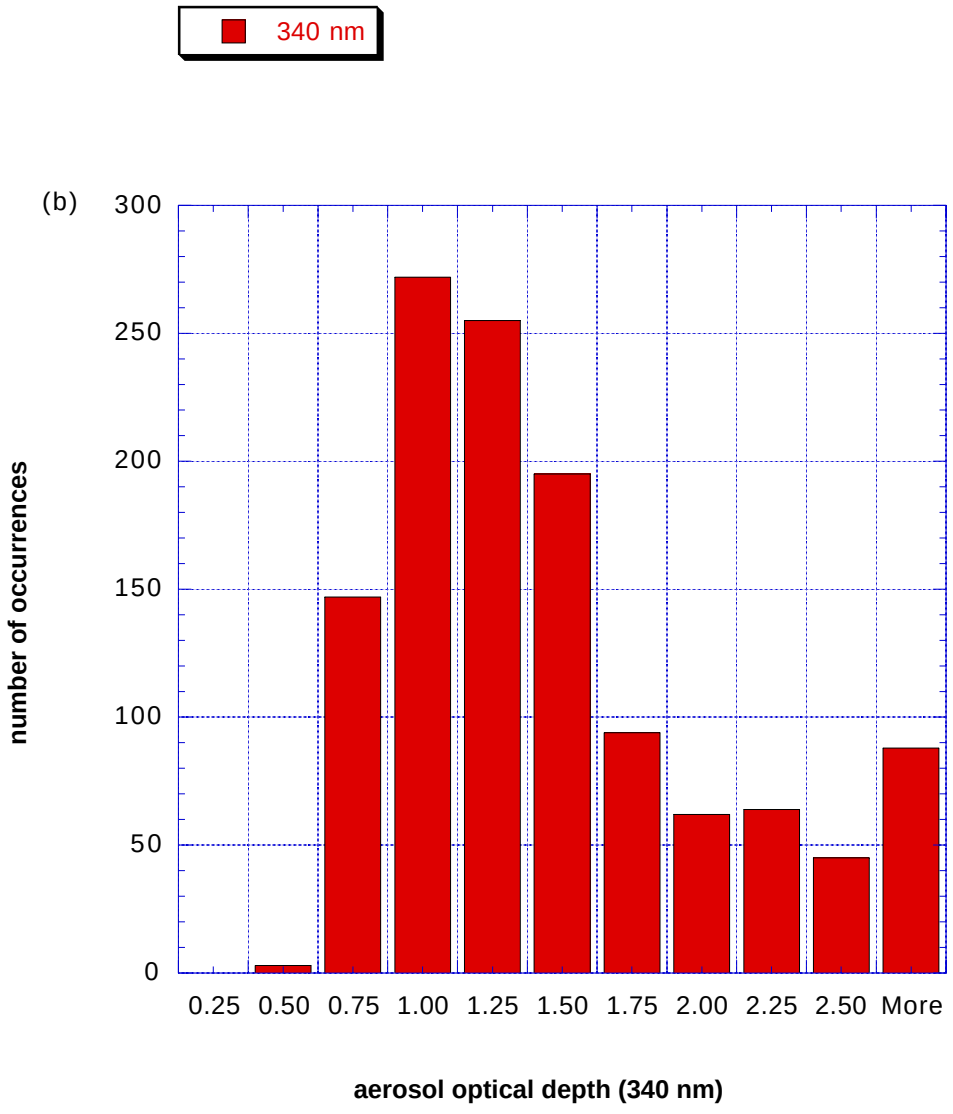
340 nm
(b)
300
250
200
150
100
50
0
number of occurrences
0.25
0.50
0.75
1.00
1.25
1.50
1.75
2.00
2.25
2.50
More
aerosol optical depth (340 nm)

Figure 5. Scattergram of parameter D versus aerosol optical depth at 500 nm from Cuiaba, Brazil and Goddard Space Flight Center observations (a) and corresponding histogram of the parameter D (b).

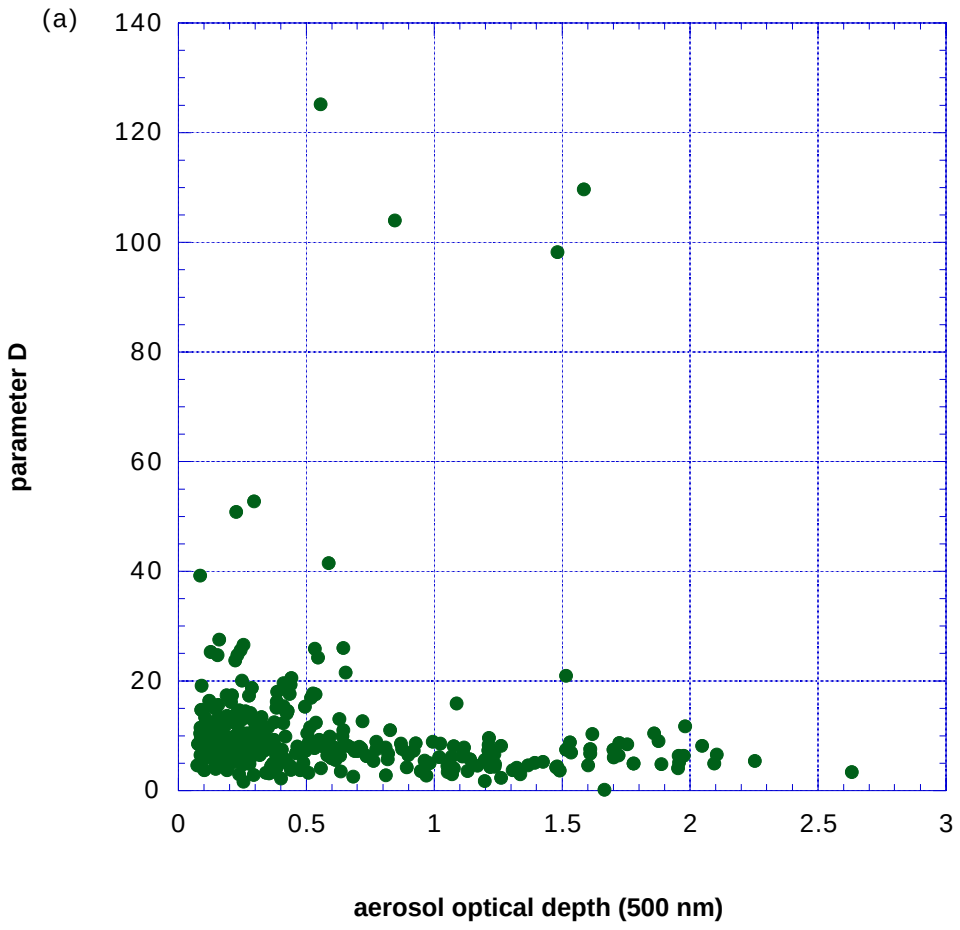

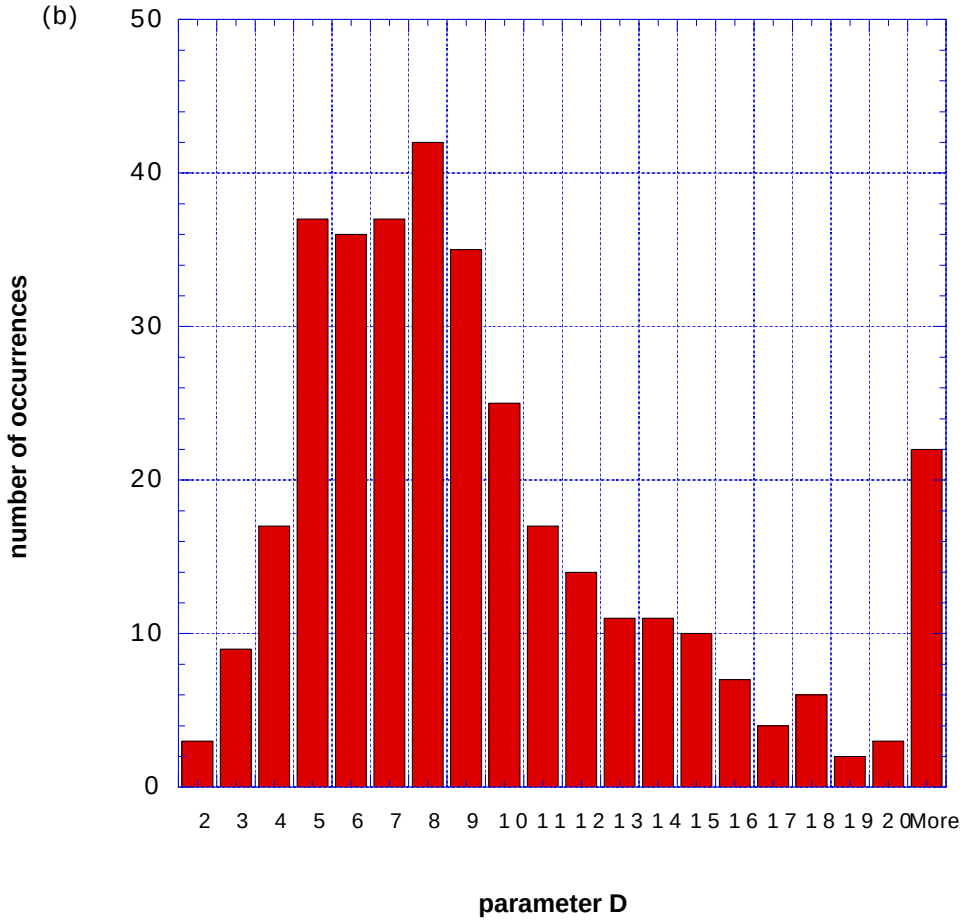
(b)
50
40
30
20
10
0
number of occurrences
2
3
4
5
6
7
8
9
10
11
12
13
14
15
16
17
18
19
20
More
parameter D

Figure 6. Histogram of the number of measurements eliminated by the smoothness criterion for observations made at Goddard Space Flight Center (a) and histogram of the corresponding change in aerosol optical depth at 500 nm (b).

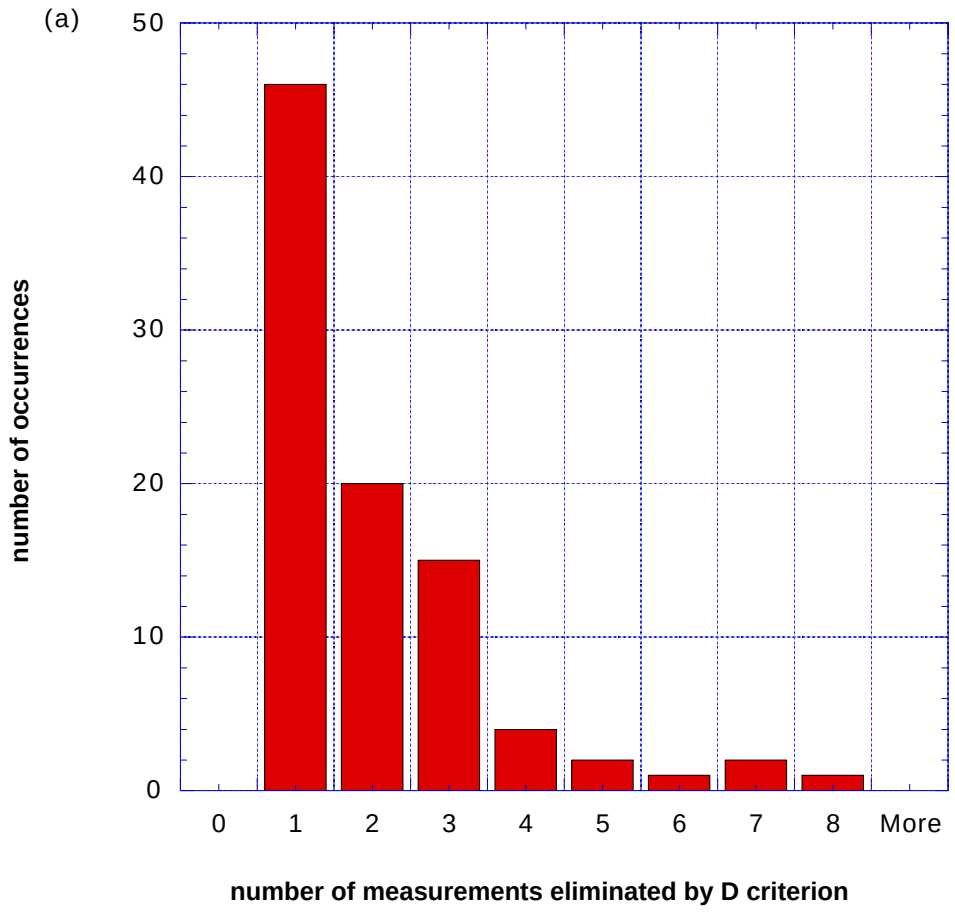

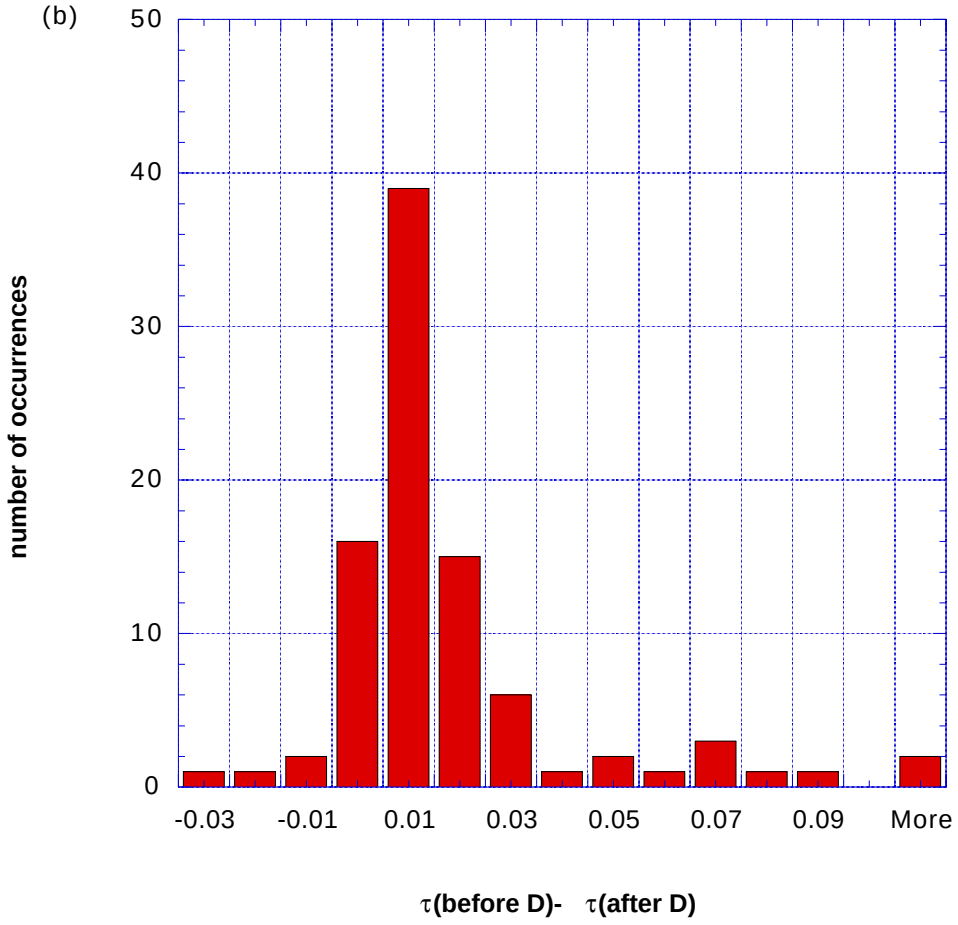
(b)
50
40
30
20
10
0
number of occurrences
-0.03
-0.01
0.01
0.03
0.05
0.07
0.09
More
τ(before D)- τ(after D)

Figure 7. Diurnal variability of aerosol optical depth on November 5, 1995 over GSFC, Greenbelt, Maryland, before (a) and after (b) screening criterion 4 (smoothness criteria) has been applied.

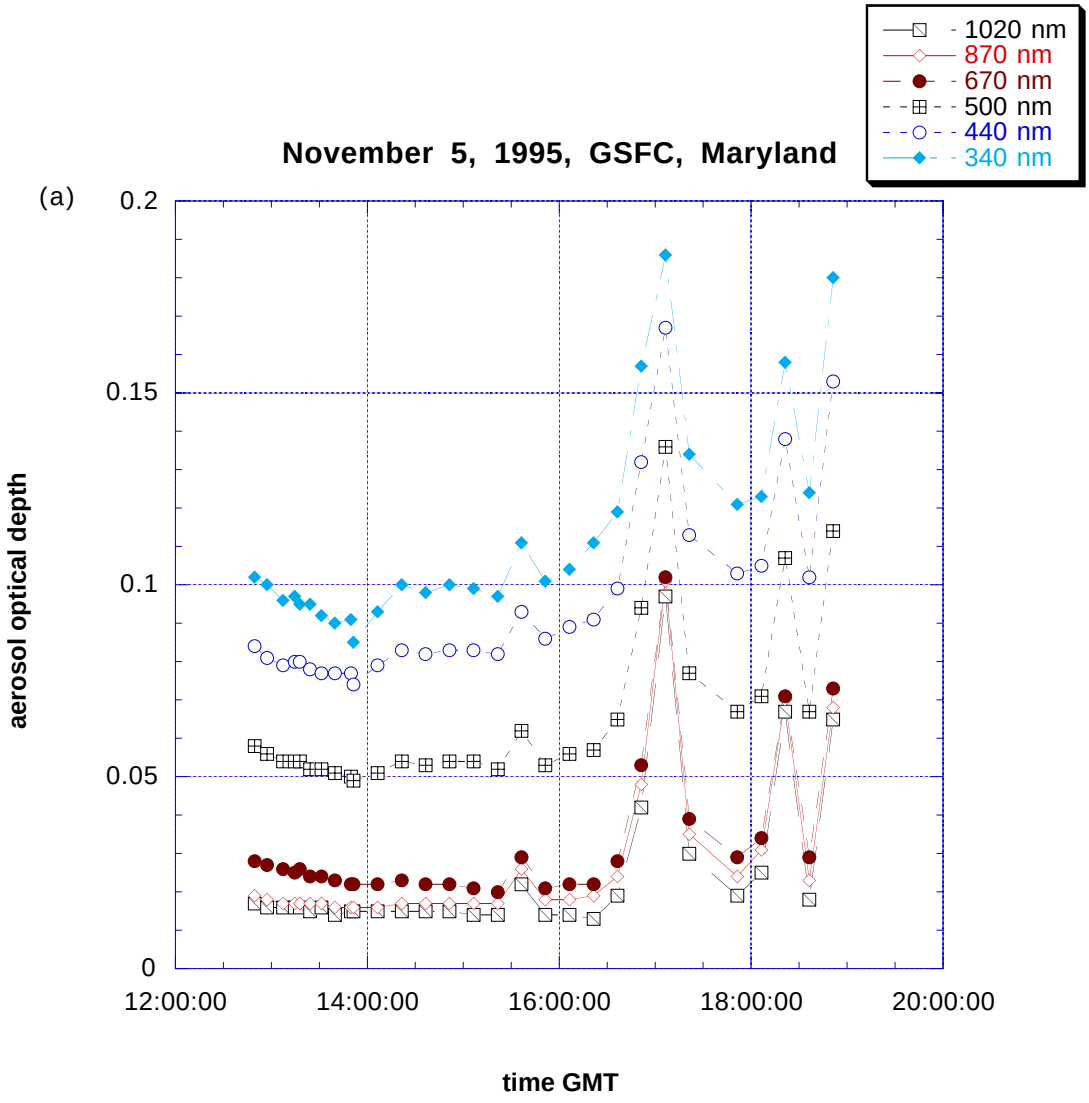

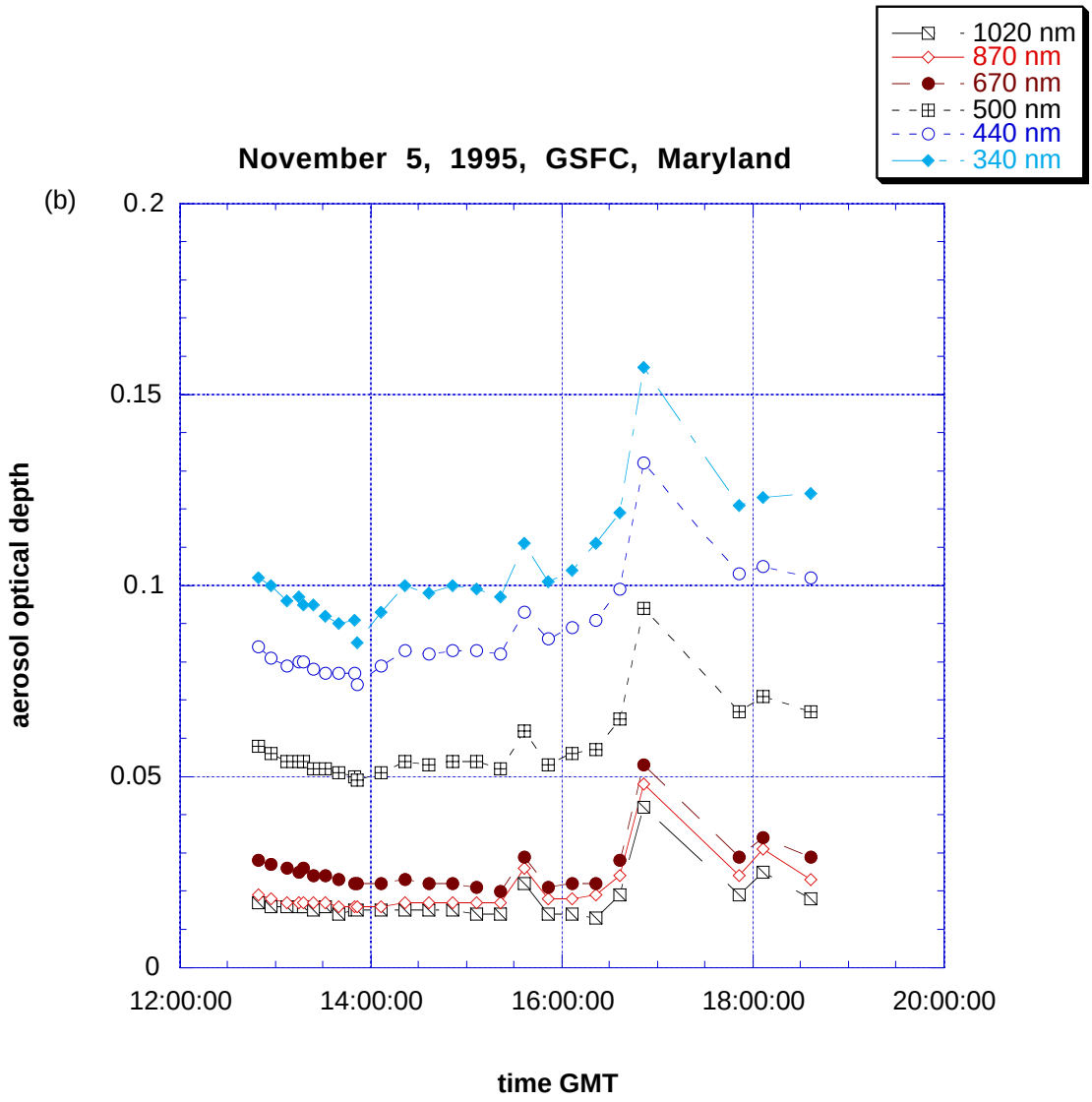
1020 nm
870 nm
670 nm
500 nm
440 nm
340 nm
November 5, 1995, GSFC, Maryland
(b)
0.2
0.15
0.1
0.05
0
aerosol optical depth
12:00:00
14:00:00
16:00:00
18:00:00
20:00:00
time GMT

Figure 8. Scattergram of the Angstrom parameter versus aerosol optical depth at 500 nm from Los Fierros, Bolivia observations before (a) and after (b) cloud-screening algorithm has been applied.

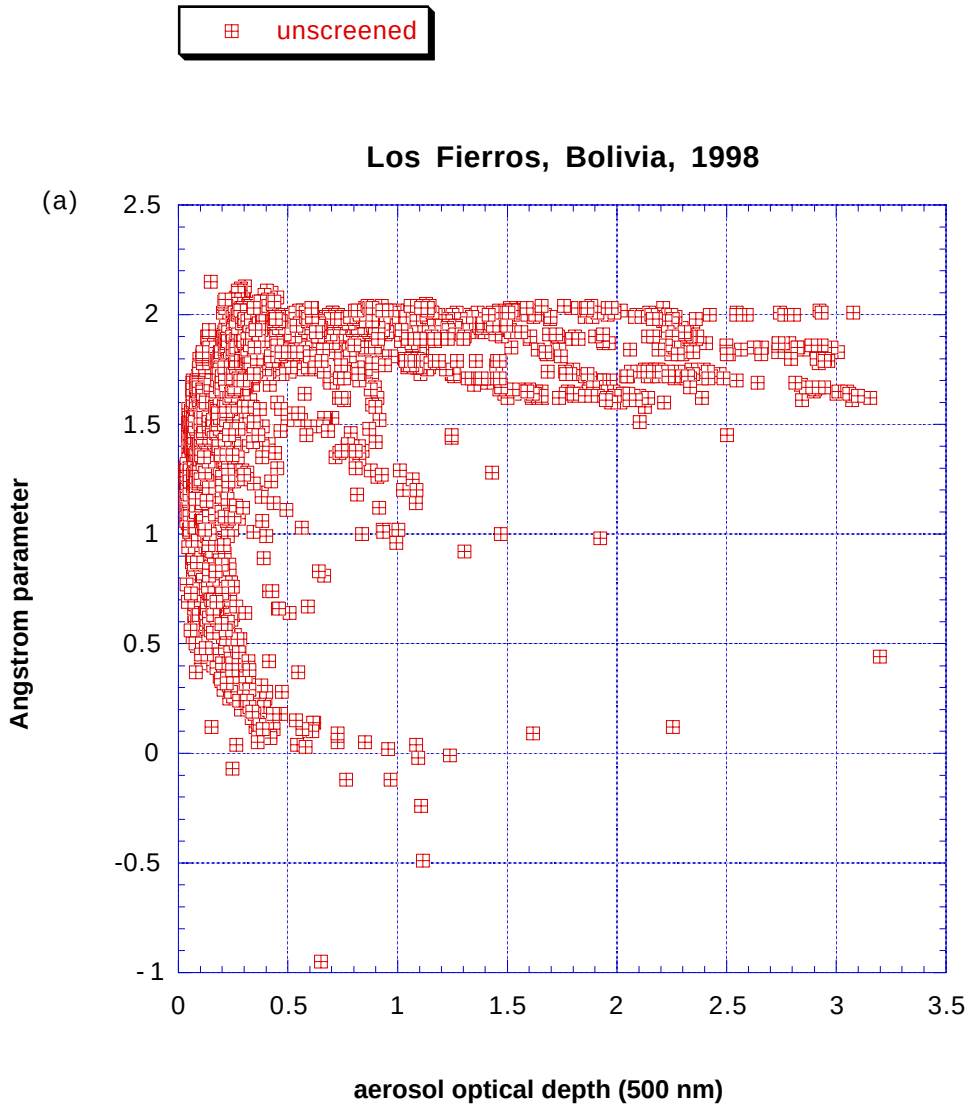

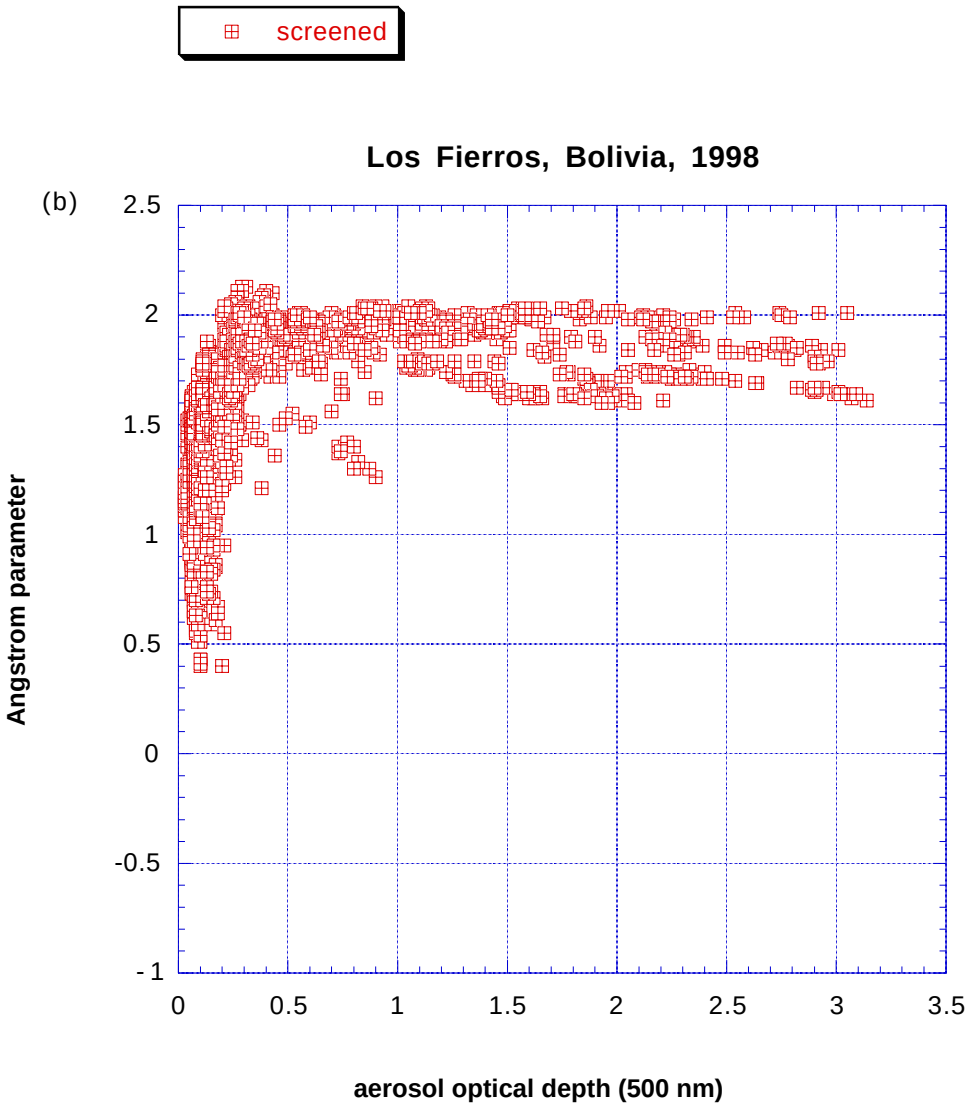
screened
Los Fierros, Bolivia, 1998
(b)
Angstrom parameter
2.5
2
1.5
1
0.5
0
-0.5
- 1
0
0.5
1
1.5
2
2.5
3
3.5
aerosol optical depth (500 nm)